

Stacked BNAS: Rethinking Broad Convolutional Neural Network for Neural Architecture Search

Zixiang Ding, Yaran Chen, Nannan Li, Dongbin Zhao

the State Key Laboratory of Management and Control for Complex Systems, Institute of Automation, Chinese Academy of Sciences, Beijing 100190, China

the School of Artificial Intelligence, University of Chinese Academy of Sciences, Beijing 100049, China
 {dingzixiang2018, chenyaran2013, linannan2017, dongbin.zhao}@ia.ac.cn

Abstract

Different from other deep scalable architecture based NAS approaches, Broad Neural Architecture Search (BNAS) proposes a broad one which consists of convolution and enhancement blocks, dubbed Broad Convolutional Neural Network (BCNN) as search space for amazing efficiency improvement. BCNN reuses the topologies of cells in convolution block, so that BNAS can employ few cells for efficient search. Moreover, multi-scale feature fusion and knowledge embedding are proposed to improve the performance of BCNN with shallow topology. However, BNAS suffers some drawbacks: 1) insufficient representation diversity for feature fusion and enhancement, and 2) time consuming of knowledge embedding design by human expert.

In this paper, we propose Stacked BNAS whose search space is a developed broad scalable architecture named Stacked BCNN, with better performance than BNAS. On the one hand, Stacked BCNN treats mini-BCNN as the basic block to preserve comprehensive representation and deliver powerful feature extraction ability. On the other hand, we propose Knowledge Embedding Search (KES) to learn appropriate knowledge embeddings. Experimental results show that 1) Stacked BNAS obtains better performance than BNAS, 2) KES contributes to reduce the parameters of learned architecture with satisfactory performance, and 3) Stacked BNAS delivers state-of-the-art efficiency of 0.02 GPU days.

1 Introduction

Neural Architecture Search (NAS) has achieved unprecedented accomplishments in structure design engineering field. However, it needs enormous computational requirements, e.g. more than 22000 GPU days for vanilla NAS (Zoph and Le 2017). A micro search space dubbed cell (Zoph et al. 2018) was proposed to mitigate the above time consuming issue. Subsequently, lots of cell-based NAS approaches were proposed to improve the efficiency further. Reinforcement Learning (RL) based ENAS (Pham et al. 2018) only needs 0.45 GPU days via parameter sharing. Gradient-based DARTS (Liu et al. 2018c) employs continuous relaxation strategy to transfer the search space from discrete to continuous, and delivers novel efficiency of 0.5 GPU days. Furthermore, PC-DARTS (Xu et al. 2020) delivers the efficiency of 0.1 GPU days via partial channel connections.

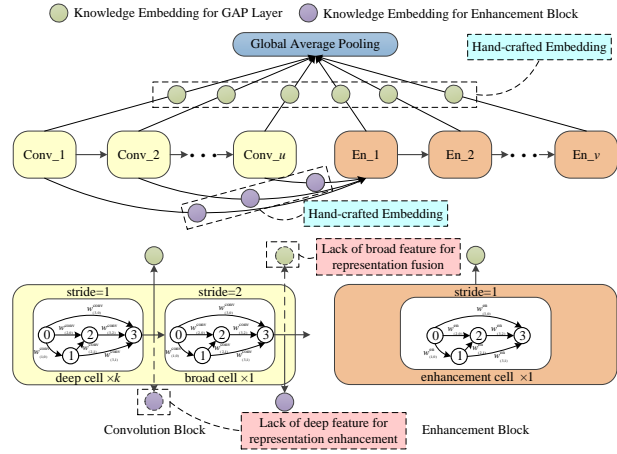


Figure 1: Issues of BCNN. 1) Lack of feature diversity for representation fusion and enhancement: only deep and broad feature informations are fed into Global Average Pooling (GAP) layer for representation fusion and the first enhancement block for representation enhancement, respectively. 2) It is extreme time consuming to design knowledge embeddings by human expert.

Different from the above NAS approaches with deep scalable architecture, BNAS (Ding et al. 2021b) proposed a broad one named Broad Convolutional Neural Network (BCNN). Benefit of BCNN, RL-based BNAS delivers state-of-the-art efficiency of 0.2 GPU days that is $2.2 \times$ faster than ENAS. However, the training mechanism of BNAS leads to terrible unfair training issue (Chu et al. 2019). BNAS-v2 (Ding et al. 2021a) was proposed to solve the unfair training issue by continuous relaxation strategy with state-of-art efficiency of 0.05 GPU days. Admittedly, BNASs achieve satisfactory performance, especially efficiency. Nevertheless, BCNN suffers two drawbacks as shown in Figure 1: 1) insufficient feature diversity for representation fusion and enhancement, and 2) hand-crafted knowledge embedding.

In this paper, we propose Stacked BNAS whose scalable architecture is named Stacked BCNN that treats mini BCNN as its basic block. Moreover, each mini BCNN can feed sufficient representations to the GAP layer and enhancement block for feature fusion and enhancement, respectively. As a

new paradigm of neural network, we also prove the universal approximation ability of Stacked BCNN. Furthermore, we transfer the knowledge embedding designing task from discrete to continuous space, and learn appropriate knowledge embeddings in a differentiable way. Our contributions can be summarized as follows:

- **Stacked BNAS:** We propose Stacked BNAS that employs Stacked BCNN as search space, to further improve the performance of NAS.
- **Stacked BCNN:** We mathematically analyse the universal approximation ability of the proposed Stacked BCNN.
- **Knowledge Embedding Search:** We also propose a differentiable algorithm for designing knowledge embedding in an automatic way.
- **Efficiency:** Contribute to the proposed Stacked BCNN and optimization algorithm, Stacked BNAS delivers state-of-the-art efficiency of 0.02 days on a single GPU.

2 Related Work

NAS consists of three components: search space, optimization strategy and estimation strategy (Elsken et al. 2019). Search space refers to not only primitive operators, but also the combination paradigm of those candidate operations (He, Zhao, and Chu 2021). There are mainly four types of search space: entire-structured (Zoph and Le 2017), cell-based (Zoph et al. 2018; Pham et al. 2018; Zhong et al. 2018), hierarchical (Liu et al. 2019; Real et al. 2019; Tan et al. 2019) and broad (Ding et al. 2021a,b).

2.1 Entire-structured Search Space

In the entire-structured search space, each layer with a specified operation (e.g. convolution, pooling) is stacked one after another (Zoph and Le 2017). Beyond that, the skip connection can be used in the above search space for exploring more complex neural architectures. This search space has two disadvantages: computationally expensive and insufficient transferability (He, Zhao, and Chu 2021).

2.2 Cell-based Search Space

To mitigate the above issues of entire-structured search space, Zoph et al. (2018) proposed cell-based search space where each cell with a list of operations is stacked one after another. Cell-based search space consists of normal and reduction cells which have different architectures and strides. Moreover, each cell treats the outputs of two predecessors as its inputs. Due to the effectiveness of cell in terms of efficiency and transferability, lots of cell-based NAS approaches were proposed, e.g. ENAS (Pham et al. 2018), DARTS (Liu et al. 2018c).

2.3 Hierarchical Search Space

Most of cell-based NAS approaches follow a two-level hierarchy: the inner cell level and the outer network level. On the one hand, the inner level chooses operation and connection of each intermediate node in the cell. On the other hand, the

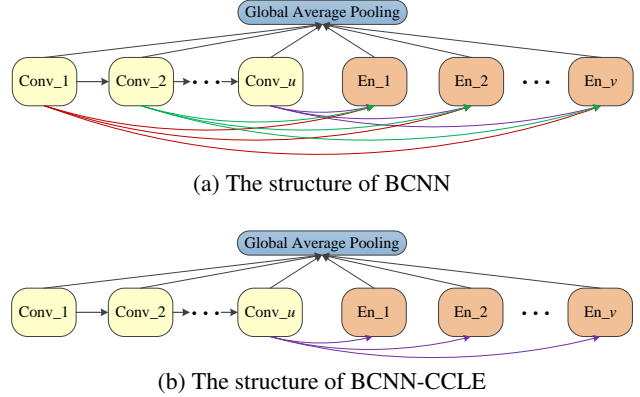


Figure 2: Broad search space (Ding et al. 2021b).

outer level controls the spatial-resolution changes. A general formulation (Liu et al. 2019) was proposed to learn the network-level structure. Liu et al. (2018b) proposed a hierarchical architecture representation to avoid manually pre-defining the network block number.

2.4 Broad Search Space

To improve the efficiency of NAS, Ding et al. (2021b) proposed a broad search space named BCNN, which employs broad topology to obtain extreme fast search speed and satisfactory performance. Actually, BCNN belongs to cell-based network-level search space. There are three broad search spaces: BCNN (see Figure 2 (a)), BCNN-CCLE (see Figure 2 (b)) and BCNN-CCE (see Figure 1). BCNNs consists of convolution and enhancement blocks which densely connect with the GAP layer for multi-scale feature fusion. The main difference among BCNNs is the connection between convolution and enhancement blocks. Similarly, Fang et al. (2020) proposed a network-level deep search space named dense search space where the MBConv (Sandler et al. 2018) is treated as its basic block rather than cell. Differently, each block of dense search space connects to several subsequent blocks.

Based on the broad search space, BNAS (Ding et al. 2021b) delivers novel efficiency of 0.2 GPU days via RL. However, BNAS suffers from the unfair training issue so that its optimization mechanism does not take full advantages of broad search space, i.e. the efficiency improvement is limited. Furthermore, a differentiable over-parameterized broad search space was proposed to solve the unfair training issue in BNAS-v2 (Ding et al. 2021a). Experimental results show that BCNN can deliver state-of-the-art search efficiency of 0.05 GPU days when its all advantages works.

3 Stacked Broad Neural Architecture Search

3.1 Search Space: Stacked Broad Convolutional Neural Network

To improve the feature diversity, we propose Stacked BCNN that treats mini BCNN as its basic block. The structures of mini BCNN and Stacked BCNN are shown in Figure 3.

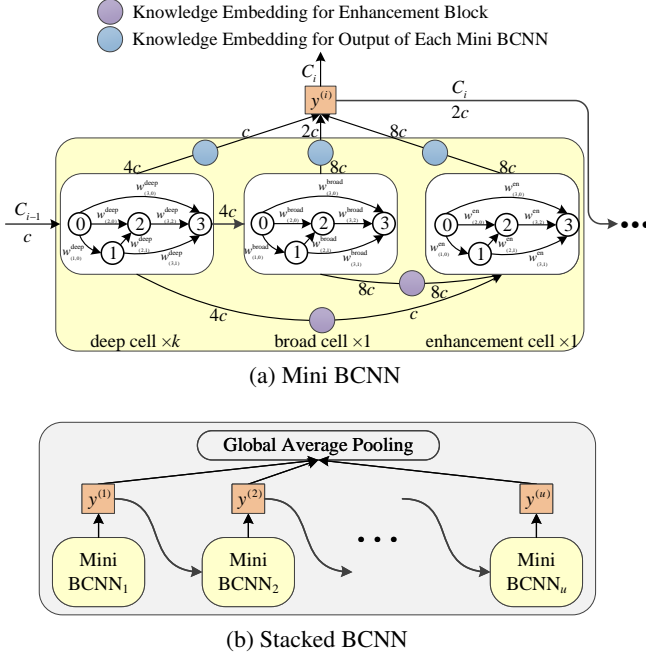


Figure 3: Search space of Stacked BNAs.

Mini BCNN Figure 3 (a) shows the structure of mini BCNN. Mini BCNN consists of $k + 1$ convolution cells (k 1-stride deep cells, single 2-stride broad cell) and 1 enhancement cell with stride 1. Deep and broad cells are used for deep and broad feature extraction, respectively. Enhancement cell treats both the outputs of deep and broad cells as inputs to obtain comprehensive enhancement representation. Furthermore, a family of 1×1 convolutions is inserted into fixed locations as the knowledge embeddings.

There are mainly two differences between BCNN and Stacked BCNN: 1) the output of each mini BCNN is the combination of all outputs of three cells rather than the output of deep cell, and 2) enhancement cell treats the outputs of convolution cells as inputs. The above two differences provide sufficient feature diversities to the GAP layer and enhancement block for representation fusion and enhancement, so that better performance can be obtained.

Stacked BCNN As shown in Figure 3 (b), the proposed Stacked BCNN consists of u mini BCNNs, where u is determined by the input size of the first mini BCNN (mini BCNN₁). To preserve the multi-scale fusion ability of vanilla BCNN, we feed the output of each mini BCNN into GAP layer.

Mathematical Information Flow We employ a 3×3 convolution as the stem layer of Stacked BCNN, and its output is treated as the two inputs of the first deep cell of mini BCNN₁, denoted as $y_{-1}^{(1)}$ and $y_0^{(1)}$.

For mini BCNN_i ($i = 1, 2, \dots, u$), its output $y^{(i)}$ can be obtained by the outputs of three cells:

$$y^{(i)} = \phi(\delta_{do}^{(i)}(y_k^{(i)}), \delta_{bo}^{(i)}(y_{k+1}^{(i)}), \delta_{eo}^{(i)}(y_{k+2}^{(i)})), \quad (1)$$

where, ϕ and $\delta_{*o}^{(i)}$ are concatenation for channel dimension and knowledge embeddings with respect to mini BCNN_i's output. Moreover, $y_k^{(i)}$ is the output of last deep cell with a list of operations φ_d that can be computed by

$$y_k^{(i)} = \varphi_d(y_{k-2}^{(i)}, y_{k-1}^{(i)}; \mathbf{W}_d^{(i)}, \mathbf{\theta}_d^{(i)}), \quad (2)$$

$y_{k+1}^{(i)}$ is the output of broad cell with a list of operations φ_b that can be obtained by

$$y_{k+1}^{(i)} = \varphi_b(y_{k-1}^{(i)}, y_k^{(i)}; \mathbf{W}_b^{(i)}, \mathbf{\theta}_b^{(i)}), \quad (3)$$

and $y_{k+2}^{(i)}$ is the output of enhancement cell with a list of operations φ_e that can be calculated by

$$y_{k+2}^{(i)} = \varphi_e(\delta_{de}^{(i)}(y_k^{(i)}), \delta_{be}^{(i)}(y_{k+1}^{(i)}); \mathbf{W}_e^{(i)}, \mathbf{\theta}_e^{(i)}), \quad (4)$$

where, $\mathbf{W}_*^{(i)}$ and $\mathbf{\theta}_*^{(i)}$ are the weight and bias matrices of corresponding cells in mini BCNN_i, $\delta_{*e}^{(i)}$ represents knowledge embeddings with respect to enhancement cell of mini BCNN_i.

The output of Stacked BCNN can be computed by

$$\mathbf{y} = \phi(y^{(1)}, y^{(2)}, \dots, y^{(u)}). \quad (5)$$

Channel Flow Graph As shown in Figure 3 (a), for mini BCNN_i, the channel number of deep cell's output can be obtained by

$$c_{deep}^{(i)} = N_{in} \times 2^{i-1} \times c, \quad i = 1, 2, \dots, u \quad (6)$$

where N_{in} represents the number of intermediate nodes, and c is the input channel number of mini BCNN₁. Moreover, the channel number of broad and enhancement cells' outputs are both $2 \times c_{deep}^{(i)}$. For those direct-connected cells and output node (e.g. broad and enhancement cells, enhancement cell and output node), corresponding knowledge embedding not reduce its feature significance. However, the significances of indirect-connected features are reduced by a quarter as shown in Figure 4 (a).

3.2 Knowledge Embedding Search (KES)

Over-parameterized Knowledge Embedding Module For each embedding on indirect edge, we construct an over-parameterized module as shown in Figure 4 (b), to discover appropriate knowledge embeddings.

We assume that c_e channels are fed into the indirect-connected embedding. The over-parameterized knowledge embedding consists of n embeddings with 2^i ($i = 1, 2, \dots, n$) output channels and a single embedding with c_e output channels, where n is the largest power of 2 less than c_e determined by

$$\operatorname{argmax}_n 2^n \quad \text{s.t. } 2^n < c_e. \quad (7)$$

Subsequently, the output of over-parameterized knowledge embedding module y_e is the channel-dimension concatenation of weighted $n + 1$ embeddings' outputs as

$$y_e = \phi(\gamma_1 y_e^{(1)}, \gamma_2 y_e^{(2)}, \dots, \gamma_{n+1} y_e^{(n+1)}), \quad (8)$$

where $y_e^{(l)}$ and γ_l ($l = 1, 2, \dots, n + 1$) represent the output and weight of l -th embedding, respectively.

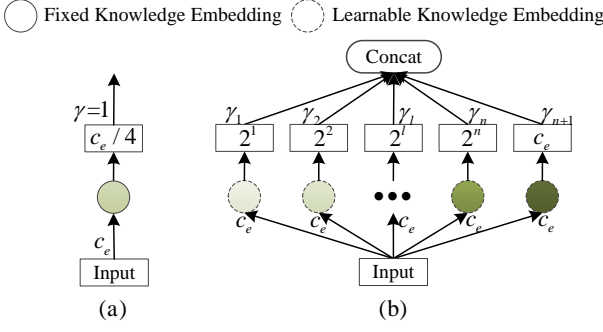


Figure 4: Embedding between indirect-connected cells and output node. (a) Hand-crafted knowledge embedding and (b) over-parameterized knowledge embedding module.

Learning Strategy After over-parameterized knowledge embedding module construction, we aim to jointly optimize the embedding weights γ and network weights w . The goal of KES is to discover γ^* that minimizes the validation loss $\mathcal{L}_{val}(w^*, \gamma^*)$, where w^* is obtained by minimizing the training loss $\mathcal{L}_{train}(w, \gamma)$. The bilevel optimization problem with lower-level variable w and upper-level variable γ can be represented as

$$\begin{aligned} \min_{\gamma} \quad & \mathcal{L}_{val}(w^*(\gamma), \gamma), \\ \text{s.t.} \quad & w^*(\gamma) = \operatorname{argmin}_w \mathcal{L}_{train}(w, \gamma). \end{aligned} \quad (9)$$

The optimization of (9) exactly is prohibitive due to $w^*(\gamma)$ needs to be recomputed by the second term of (9) whenever γ takes any change (Liu et al. 2018c). Therefore, we propose an approximate iterative optimization process as follows. For each gradient descent step, network weights w and embedding weights γ are optimized by alternating in the weight and embedding spaces, respectively. At step t , given the current embedding γ_{t-1} , we update w_t by descending the training loss $\mathcal{L}_{train}(w_{t-1}, \gamma_{t-1})$. Subsequently, we keep w_t fixing and optimize the over-parameterized knowledge embedding module with learning rate ξ by descending

$$\nabla_{\gamma} \mathcal{L}_{val}(w_t - \xi \nabla_w \mathcal{L}_{train}(w_t, \gamma_{t-1}), \gamma_{t-1}). \quad (10)$$

At last, we replace every over-parameterized knowledge embedding module as the knowledge embedding with largest weight by taking argmax.

3.3 Optimization Algorithm

The optimization algorithm is shown in **Algorithm 1**.

Continuous Relaxation In mini BCNN, each cell consists of 2 input nodes $\{x_{(0)}, x_{(1)}\}$, $N - 3$ intermediate nodes $\{x_{(2)}, \dots, x_{(N-2)}\}$ and a single output node $\{x_{(N-1)}\}$. Each intermediate node $x_{(i)}$ can be computed by

$$x_{(i)} = \sum_{j < i} o_{(i,j)}(x_{(j)}), \quad (11)$$

where, $o_{(i,j)}$ is the operator between $x_{(i)}$ and $x_{(j)}$ chosen from candidate operation set \mathcal{O} . Moreover, the outputs of

Algorithm 1: Stacked BNAs

```

1 Define  $p$  as the early stopping epoch number,  $q$  as the
stable epoch number with zero initialization,  $kes$  as
the flags represented using KES or not,  $arch_{prev}$  as
previous architecture with None initialization;
2 For each edge  $(i, j)$ , use (13) and (14) for continuous
relaxation as  $f_{(i,j)}^{PC}(x_{(j)}^{PC}; M_{(i,j)})$  parameterized by
 $\alpha_{(i,j)}$  and  $\beta_{(i,j)}$ ;
3 Define architecture weight set  $\Theta = [\alpha, \beta]$ ;
4 if  $kes$  then
5   Use (7) and (8) to construct over-parameterized
   knowledge embedding module parameterized
   by  $\gamma$ ;
6    $\Theta = [\alpha, \beta, \gamma]$ ;
7 end
8 while not converged do
9   Optimize  $w$  by descending  $\nabla_w \mathcal{L}_{train}(w, \Theta)$ ;
10  Optimize  $\Theta$  by descending
     $\nabla_{\Theta} \mathcal{L}_{val}(w - \xi \nabla_w \mathcal{L}_{train}(w, \Theta), \Theta)$ ;
11  Determine current architecture  $arch_{curr}$  by
    taking argmax;
12   $arch_{prev} = arch_{curr}$ ;
13  if  $arch_{curr} == arch_{prev}$  then
14     $q = q + 1$ ;
15    if  $q \geq p$  then
16      break
17    end
18  else
19     $q = 1$ ;
20  end
21 end
22 Output  $arch_{curr}$  as the best architecture.

```

all intermediate nodes are employed to deliver $x_{(N-1)}$ by channel-dimension concatenation.

Subsequently, the over-parameterized Stacked BCNN is constructed by the strategy of continuous relaxation (Liu et al. 2018c). Particularly, we relax edge (i, j) of each cell for mini BCNN by

$$f_{(i,j)}(x_{(j)}) = \sum_{o \in \mathcal{O}} \frac{\exp(\alpha_{(i,j)}^o)}{\sum_{o' \in \mathcal{O}} \exp(\alpha_{(i,j)}^{o'})} o(x_{(j)}), \quad (12)$$

where, operation $o(\cdot)$ is weighted by architecture weight α^o .

Partial Channel Connections (PCC) We employ PCC (Xu et al. 2020) to improve the memory efficiency of Stacked BNAs. The continuous relaxation of Stacked BNAs with PCC can be obtained by

$$\begin{aligned} f_{(i,j)}^{PC}(x_{(j)}; M_{(i,j)}) = & \sum_{o \in \mathcal{O}} \frac{\exp(\alpha_{(i,j)}^o)}{\sum_{o' \in \mathcal{O}} \exp(\alpha_{(i,j)}^{o'})} o(M_{(i,j)} * x_{(j)}) \\ & + (1 - M_{(i,j)}) * x_{(j)}, \end{aligned} \quad (13)$$

where, $M_{(i,j)}$ represents mask of channel sample whose values are chosen from $\{0, 1\}$.

Moreover, we employ edge normalization to mitigate the undesired fluctuation in search phase via $\beta_{(i,j)}$ as

$$x_{(i)}^{PC} = \sum_{j < i} \frac{\exp(\beta_{(i,j)})}{\sum_{j' < i} \exp(\beta_{(i,j')})} \cdot f_{(i,j)}(x_{(j)}). \quad (14)$$

At last, each operation of best architecture is obtained by

$$o_{(i,j)} = \operatorname{argmax}_{o \in \mathcal{O}} \frac{\exp(\alpha_{(i,j)}^o)}{\sum_{o' \in \mathcal{O}} \exp(\alpha_{(i,j)}^{o'})} \cdot \frac{\exp(\beta_{(i,j)})}{\sum_{j' < i} \exp(\beta_{(i,j')})}. \quad (15)$$

Early Stopping As described in DARTS+ (Liang et al. 2019), there are two indices for early stopping: 1) the number of *skip connection* and 2) the number of stable epochs. On the one hand, the search procedure will be stopped when there are more than one *skip connection* in one cell, for avoiding the performance collapse issue. PCC contributes to reduce the predominance of *skip connection*, so that we do not choose the first index in this paper. On the other hand, the search procedure will be stopped when the ranking of architecture weights is no longer changed for a determined number of epochs. This index means that the search procedure stops when arriving at a saturated state. Above all, the second index is chosen for early stopping of Stacked BNAS using the following criterion:

Criterion 1: Stop search procedure when the ranking of architecture weights is no longer changed for three epochs.

4 Universal Approximation Ability of Stacked BCNN

Given the initial input channel number c , the output of mini BCNN $_i$ with C_i channels, i.e. (1) can be rewritten as

$$y^{(i)} = \phi(\mathbf{x}; \{\delta^{(i)}, \varphi^{(i)}, \mathbf{W}_d^{(i)}, \boldsymbol{\theta}_d^{(i)}, \mathbf{W}_b^{(i)}, \boldsymbol{\theta}_b^{(i)}, \mathbf{W}_e^{(i)}, \boldsymbol{\theta}_e^{(i)}\}), \quad (16)$$

where \mathbf{x} represents input data. After GAP, each channel of $y^{(i)}$ is transformed into a single-pixel neuron-like feature map, so that we can treat it as C_i neurons.

Given standard hypercube $\mathbf{I}^d = [0; 1]^d \in \mathbb{R}^d$ and any continuous function $f \in C(\mathbf{I}^d)$, the proposed Stacked BCNN can be equivalently represented as

$$f_{\mathbf{p}_{k,u}} = \sum_{z=1}^Z w_z \sigma(\mathbf{x}; \{\phi, \delta, \varphi, \mathbf{W}^{(1)}, \boldsymbol{\theta}^{(1)}, \dots, \mathbf{W}^{(u)}, \boldsymbol{\theta}^{(u)}\}), \quad (17)$$

where, $Z = \sum_{i=1}^u C_i$ is the neuron number of GAP's output, w represents the weight of fully connected layer, $\mathbf{p}_{k,u} = (k, u, c, w_1, \dots, w_Z, \mathbf{W}, \boldsymbol{\theta})$ represents the set of overall parameters for Stacked BCNN, σ is the activation function. Given the probability measure $\zeta_{k,u}$, we define randomly generated variables on it as $\xi_{k,u} = (w_1, \dots, w_Z, \mathbf{W}, \boldsymbol{\theta})$. For compact set Ω of \mathbf{I}^d , the distance between any continuous function and Stacked BCNN can be calculated as

$$\chi_{\Omega}(f, f_{\mathbf{p}_{k,u}}) = \sqrt{\mathbb{E} \left[\int_{\Omega} (f(\mathbf{x}) - f_{\mathbf{p}_{k,u}}(\mathbf{x}))^2 d\mathbf{x} \right]}. \quad (18)$$

Based on the above hypotheses, a theorem with proof of Stacked BCNN is given as below.

Theorem 1: Given any continuous function $f \in C(\mathbf{I}^d)$ and any compact set $\Omega \in \mathbf{I}^d$, Stacked BCNN with nonconstant bounded functions ϕ, δ, φ , and absolutely integrable activation function σ whose definition domain is \mathbf{I}^d so that $\int_{\mathbb{R}^d} \sigma^2(\mathbf{x}) d\mathbf{x} < \infty$, has a sequence of $\{f_{\mathbf{p}_{k,u}}\}$ with probability measures $\zeta_{k,u}$ satisfied that

$$\lim_{u \rightarrow \infty} \chi_{\Omega}(f, f_{\mathbf{p}_{k,u}}) = 0. \quad (19)$$

Moreover, the trainable parameters $\xi_{k,u}$ is generated by $\zeta_{k,u}$.

Proof: Define input data \mathbf{x} , nonconstant bounded functions ϕ, δ, φ , approximation function $f_{\mathbf{p}_{k,u'}}$ of Stacked BCNN with u' mini BCNNs, probability distribution $\zeta_{k,u'}$ for trainable parameters generation, the weight matrix of fully connected layer $\mathbf{w}' = [w'_1, \dots, w'_{Z'}]^T$ where $Z' = \sum_{z=1}^{u'} C_z$ and supplement weight $\mathbf{w}'' = [w''_1, \dots, w''_{C_{u'+1}}]^T$.

For Stacked BCNN with u' (any integer) mini BCNNs, we compute its output by

$$f_{\mathbf{w}'} = \sum_{z=1}^{Z'} w'_z \sigma(\mathbf{x}; \{\phi, \delta, \varphi, \mathbf{W}^{(1)}, \boldsymbol{\theta}^{(1)}, \dots, \mathbf{W}^{(u')}, \boldsymbol{\theta}^{(u')}\}). \quad (20)$$

Subsequently, Stacked BCNN with input data \mathbf{x} can approximate continuous function f with bounded and integrable resident function $f_{r_{u'}}$ in \mathbf{I}^d as

$$f_{r_{u'}}(\mathbf{x}) = f(\mathbf{x}) - f_{\mathbf{w}'}(\mathbf{x}). \quad (21)$$

As described in previous work (Rudin 2006), for $\forall \varepsilon > 0$, a function $f_{b_{u'}}$ in $C(\mathbf{I}^d)$ always can be found to satisfy the following expression as

$$\chi_{\Omega}(f_{b_{u'}}, f_{r_{u'}}) < \frac{\varepsilon}{2}. \quad (22)$$

We define an extra mini BCNN (i.e. mini BCNN $_{u'+1}$) to approximate $f_{b_{u'}}$ with $C_{u'+1}$ channels. Mini BCNN $_{u'+1}$ can be equivalently expressed as

$$f_{\mathbf{w}''} = \sum_{z=1}^{C_{u'+1}} w''_z \underbrace{\sigma(\mathbf{x}; \{\phi, \delta, \varphi, \mathbf{W}^{(u'+1)}, \boldsymbol{\theta}^{(u'+1)}\})}_{\vartheta}, \quad (23)$$

Similarly, we can conclude that the composition function ϑ in (23) is absolutely integrable. According to *Theorem 1* in (Igelnik and Pao 1995), for $\forall \varepsilon > 0$, a sequence of $f_{\mathbf{w}''}$ can be found to satisfy the following expression as

$$\chi_{\Omega}(f_{b_{u'}}, f_{\mathbf{w}''}) < \frac{\varepsilon}{2}. \quad (24)$$

Moreover, the output of Stacked BCNN can be rewritten as

$$f_{\mathbf{p}_{k,u}} = f_{\mathbf{w}'} + f_{\mathbf{w}''}. \quad (25)$$

Above all, we can obtain the distance between f and $f_{\mathbf{p}_{k,u}}$

by

$$\begin{aligned}
\chi_{\mathbf{I}^d}(f, f_{\mathbf{p}_{k,u}}) &= \sqrt{\mathbb{E} \left[\int_{\Omega} (f(\mathbf{x}) - f_{\mathbf{p}_{k,u}}(\mathbf{x}))^2 d\mathbf{x} \right]} \\
&= \sqrt{\mathbb{E} \left[\int_{\Omega} ((f(\mathbf{x}) - f_{\mathbf{w}'}(\mathbf{x})) - f_{\mathbf{w}''}(\mathbf{x}))^2 d\mathbf{x} \right]} \\
&= \sqrt{\mathbb{E} \left[\int_{\Omega} (f_{r_{u'}} - f_{\mathbf{w}''})^2 d\mathbf{x} \right]} \\
&= \chi_{\Omega}(f_{r_{u'}}, f_{\mathbf{w}''}) \\
&\leq \chi_{\Omega}(f_{b_{u'}}, f_{r_{u'}}) + \chi_{\Omega}(f_{b_{u'}}, f_{\mathbf{w}''}) \\
&< \frac{\varepsilon}{2} + \frac{\varepsilon}{2} \\
&< \varepsilon
\end{aligned} \tag{26}$$

Therefore, we can conclude that

$$\lim_{u,v \rightarrow \infty} \chi_{\Omega}(f, f_{\mathbf{p}_{k,u}}) = 0. \tag{27}$$

5 Experiments and Results

5.1 Datasets and Implementation Details

Datasets We employ CIFAR-10 and ImageNet to verify the effectiveness of the proposed Stacked BNAS. CIFAR-10 is a small scale image classification dataset with 32×32 pixels that contains 50K training images and 10K test images. ImageNet contains about 1.3M training data and 50K validation data with various pixels over 1000 object categories.

Implementation Details Data preprocessing technique follows BNAS-v2 for CIFAR-10 and ImageNet. We implement architecture search without or with KES. For architecture search, we repeat the implementation five times. For architecture evaluation, the mean value of three repetitive re-training experiments is treated as the index to determine the best architecture. Furthermore, the best architecture learned on CIFAR-10 is transferred to ImageNet.

5.2 Experiments on CIFAR-10

Experimental Settings As aforementioned, we will implement two experiments on CIFAR-10: 1) Stacked BNAS and 2) Stacked BNAS with KES.

For architecture search without KES, over-parameterized Stacked BCNN consists of 2 mini BCNNs where each one contains 1 broad cell and 1 enhancement cell. The batch size and network learning rate are set to 512 and 0.2, respectively. Moreover, we set the architecture learning rate to 6×10^{-4} . For architecture search with KES, over-parameterized Stacked BCNN consists of 2 mini BCNNs where each one contains 1 deep cell, 1 broad cell and 1 enhancement cell. Due to more memory requirements of KES, we set the batch size and network learning rate are set to 128 and 0.05, respectively. Beyond that, we set larger architecture learning rate 2×10^{-3} when knowledge embedding is learned. Detailed experimental settings can be found in supplementary materials.

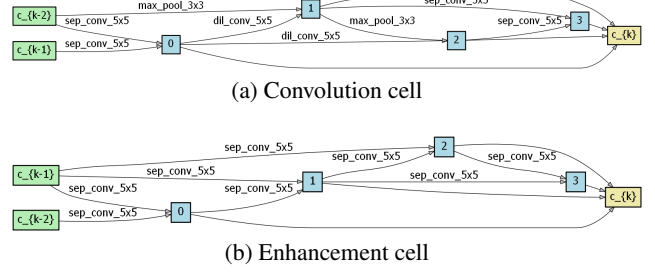


Figure 5: Architecture learned by Stacked BNAS.

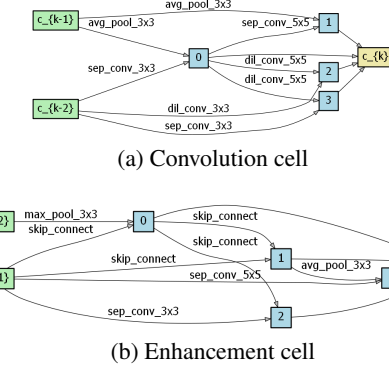


Figure 6: Architecture learned by Stacked BNAS with KES.

Table 1: Hand-crafted and learned knowledge embedding with $c = 44$ input channels.

Feature	Enhancement		Output	
	Design	Search	Design	Search
Deep ₁	c	$2 (\downarrow)$	c	$8 (\downarrow)$
Broad ₁	$4c$	$4c$	$2c$	$8c (\uparrow)$
Deep ₂	$2c$	$128 (\uparrow)$	$2c$	$64 (\downarrow)$
Broad ₂	$8c$	$8c$	$4c$	$4 (\downarrow)$

Results and Analysis For Stacked BNAS, we visualize the learned architecture in Figure 5. For Stacked BNAS with KES, we show the best architecture and embedding in Figure 6 and Table 1, respectively. Furthermore, Table 2 summarizes the comparison of the proposed Stacked BNAS with other novel NAS approaches on CIFAR-10.

Contribute to the combination of Stacked BCNN and early stopping strategy, Stacked BNAS delivers state-of-the-art efficiency of 0.02 GPU days and competitive test accuracy of 97.29% with 3.7M parameters. Beyond that, Stacked BNAS with KES discovers a Stacked BCNN with 2.78% test error and just 2.9M parameters (about 22% less than Stacked BNAS). Moreover, over-parameterized knowledge embedding module leads to more trainable parameters and memory requirements than vanilla Stacked BNAS, so that larger costs are needed. As shown in Table 1, one indirect-connected knowledge embedding of each mini BCNN has more output channels than hand-crafted one. The above knowledge embedding changes lead to parameter reduction of the architecture learned by Stacked BNAS with KES.

Table 2: Comparison of the proposed Stacked BNAs and other state-of-the-art NAS approaches on CIFAR-10.

Architecture	Error (%)	Params (M)	Search Cost (GPU days)	Number of Cells	Search Method	Topology
LEMONADE (Elsken et al. 2018)	3.05	4.7	80	-	evolution	deep
DARTS (1st order) (Liu et al. 2018c)	3.00	3.3	0.45	20	gradient-based	deep
DARTS (random) (Liu et al. 2018c)	3.49	3.1	-	20	-	deep
SNAS + mild constraint (Xie et al. 2018)	2.98	2.9	1.50	20	gradient-based	deep
P-DARTS (Chen et al. 2019)	2.50	3.4	0.30	20	gradient-based	deep
GDAS-NSAS (Zhang et al. 2020)	2.73	3.5	0.40	20	gradient-based	deep
PC-DARTS (Xu et al. 2020)	2.57	3.6	0.10	20	gradient-based	deep
ENAS (Pham et al. 2018)	2.89	4.6	0.45	17	RL	deep
BNAS-CCE (Ding et al. 2021b)	2.88	4.8	0.19	8	RL	broad
BNAS-v2 (Ding et al. 2021a)	2.79	3.7	0.05	8	gradient-based	broad
Random	3.12	3.1	-	8	-	broad
Stacked BNAs (Ours)	2.71	3.6	0.02	8	gradient-based	broad
Stacked BNAs+KES (Ours)	2.78	2.9	0.15	8	gradient-based	broad

Table 3: Comparison of the proposed Stacked BNAs and other state-of-the-art NAS approaches on ImageNet.

Architecture	Test Err. (%)		Params (M)	Search Cost (GPU days)	FLOPs (M)	Search Method	Topology
	top-1	top-5					
AmoebaNet-A (Real et al. 2019)	25.5	8.0	5.1	3150	555	evolution	deep
AmoebaNet-B (Real et al. 2019)	26.0	8.5	5.3	3150	555	evolution	deep
NASNet-A (Zoph et al. 2018)	26.0	8.4	5.3	1800	564	RL	deep
NASNet-B (Zoph et al. 2018)	27.2	8.7	5.3	1800	488	RL	deep
PNAS (Liu et al. 2018a)	25.8	8.1	5.1	225	588	SMBO	deep
DARTS (2nd order) (Liu et al. 2018c)	26.7	8.7	4.7	1.50	574	gradient-based	deep
SNAS (mild) (Xie et al. 2018)	27.3	9.2	4.3	1.50	522	gradient-based	deep
P-DARTS (Chen et al. 2019)	24.4	7.4	4.9	0.30	557	gradient-based	deep
PC-DARTS (Xu et al. 2020)	25.1	7.8	5.3	0.10	586	gradient-based	deep
BNAS-v2 (Ding et al. 2021a)	27.0	10.5	4.6	0.19	576	gradient-based	broad
Stacked BNAs (Ours)	26.4	8.9	4.7	0.02	485	gradient-based	broad

Compared with those NAS approaches with deep topology, Stacked BNAs obtains best efficiency and competitive accuracy. In terms of random architecture, Stacked BCNN obtains 0.38% better accuracy than DARTS used which further examines the effectiveness of the proposed Stacked BCNN. Furthermore, Stacked BNAs is 5 \times faster than PC-DARTS whose efficiency ranks the best. Compared with BNAs, the proposed Stacked BNAs delivers better efficiency and accuracy. On the one hand, the efficiency of Stacked BNAs is about 10 \times and 2.5 \times faster than BNAs-v1 and BNAs-v2, respectively. On the other hand, the accuracy of Stacked BNAs is about 0.2% and 0.1% better than BNAs-v1 and BNAs-v2, respectively. Stacked BNAs with KES can deliver better accuracy with about 22% and 36% parameter reduction, respectively.

5.3 Experiments on ImageNet

Experimental Settings In order to transfer the architecture learned by Stacked BNAs on ImageNet, we treat three 3 \times 3 convolutions as stem layers that reduce the input size from 224 \times 224 to 28 \times 28. Subsequently, a Stacked BCNN is constructed by 2 mini BCNNs where each one contains 2 deep cells, 1 broad cell and 1 enhancement cell. Detailed

experimental settings are shown in supplementary materials.

Results and Analysis Table 3 summarizes the comparison of the proposed Stacked BNAs with other novel NAS approaches on ImageNet.

Compared with previous impactful NAS approaches (e.g. AmoebaNet, NASNet, PNAS), the proposed Stacked BNAs delivers competitive or better performance with state-of-the-art efficiency of 0.02 GPU days which is 5 or 6 magnitudes faster. For those efficient NAS approaches (e.g. DARTS, SNAS, PC-DARTS), Stacked BNAs also obtains competitive or better performance with 1 or 2 magnitudes faster efficiency. Compared with BNAs-v2, Stacked BNAs obtains better performance in terms of top-1 and top-5 accuracy. As aforementioned, the main difference between BNAs-v2 and the proposed Stacked BNAs is broad scalable architecture, so that the effectiveness of Stacked BCNN can be promised. Moreover, the efficiency of BNAs-v2 is 4.5 \times slower than Stacked BNAs.

6 Conclusions

This paper proposes Stacked BNAs whose scalable architecture named Stacked BCNN can provide more feature diversities for representation fusion and enhancement than

vanilla one. A differentiable algorithm is also proposed to learn appropriate knowledge embedding for Stacked BCNN in an automatic way. Contribute to the combination of Stacked BCNN and efficient optimization algorithm, the proposed Stacked BNAS delivers state-of-the-art efficiency of 0.02 GPU days with competitive performance.

References

Chen, X.; Xie, L.; Wu, J.; and Tian, Q. 2019. Progressive differentiable architecture search: Bridging the depth gap between search and evaluation. In *Proceedings of the IEEE International Conference on Computer Vision (ECCV)*, 1294–1303.

Chu, X.; Zhang, B.; Xu, R.; and Li, J. 2019. Fairnas: Rethinking evaluation fairness of weight sharing neural architecture search. *arXiv preprint arXiv:1907.01845*.

Ding, Z.; Chen, Y.; Li, N.; and Zhao, D. 2021a. BNAs-v2: Memory-efficient and performance-collapse-prevented broad neural architecture search. *IEEE Transactions on Systems, Man, and Cybernetics: Systems*.

Ding, Z.; Chen, Y.; Li, N.; Zhao, D.; Sun, Z.; and Chen, C. P. 2021b. BNAs: Efficient Neural Architecture Search Using Broad Scalable Architecture. *IEEE Transactions on Neural Networks and Learning Systems*.

Elsken, T.; Metzen, J. H.; Hutter, F.; et al. 2018. Efficient multi-objective neural architecture search via Lamarckian evolution. In *International Conference on Learning Representations (ICLR)*.

Elsken, T.; Metzen, J. H.; Hutter, F.; et al. 2019. Neural architecture search: A survey. *Journal of Machine Learning Research*, 20: 1–21.

Fang, J.; Sun, Y.; Zhang, Q.; Li, Y.; Liu, W.; and Wang, X. 2020. Densely connected search space for more flexible neural architecture search. In *Proceedings of the IEEE Conference on Computer Vision and Pattern Recognition (CVPR)*, 10628–10637.

He, X.; Zhao, K.; and Chu, X. 2021. AutoML: A Survey of the State-of-the-Art. *Knowledge-Based Systems*, 212: 106622.

Igelnik, B.; and Pao, Y. 1995. Stochastic choice of basis functions in adaptive function approximation and the functional-link net. *IEEE Transactions on Neural Networks*, 6(6): 1320–1329.

Liang, H.; Zhang, S.; Sun, J.; He, X.; Huang, W.; Zhuang, K.; and Li, Z. 2019. Darts+: Improved differentiable architecture search with early stopping. *arXiv preprint arXiv:1909.06035*.

Liu, C.; Chen, L.-C.; Schroff, F.; Adam, H.; Hua, W.; Yuille, A. L.; and Fei-Fei, L. 2019. Auto-deeplab: Hierarchical neural architecture search for semantic image segmentation. In *Proceedings of the IEEE conference on Computer Vision and Pattern Recognition (CVPR)*, 82–92.

Liu, C.; Zoph, B.; Neumann, M.; Shlens, J.; Hua, W.; Li, L.; FeiFei, L.; Yuille, A.; Huang, J.; and Murphy, K. 2018a. Progressive neural architecture search. In *Proceedings of the European Conference on Computer Vision (ECCV)*, 19–34.

Liu, H.; Simonyan, K.; Vinyals, O.; Fernando, C.; and Kavukcuoglu, K. 2018b. Hierarchical Representations for Efficient Architecture Search. In *International Conference on Learning Representations (ICLR)*.

Liu, H.; Simonyan, K.; Yang, Y.; et al. 2018c. DARTS: Differentiable architecture search. In *International Conference on Learning Representations (ICLR)*.

Pham, H.; Guan, M.; Zoph, B.; Le, Q.; and Dean, J. 2018. Efficient neural architecture search via parameters sharing. In *International Conference on Machine Learning (ICLR)*, 4095–4104.

Real, E.; Aggarwal, A.; Huang, Y.; and Le, Q. V. 2019. Regularized evolution for image classifier architecture search. In *Proceedings of the AAAI Conference on Artificial Intelligence (AAAI)*, volume 33, 4780–4789.

Rudin, W. 2006. *Real and complex analysis*. Tata McGraw-hill education.

Sandler, M.; Howard, A.; Zhu, M.; Zhmoginov, A.; and Chen, L.-C. 2018. Mobilenetv2: Inverted residuals and linear bottlenecks. In *Proceedings of the IEEE Conference on Computer Vision and Pattern Recognition (CVPR)*, 4510–4520.

Tan, M.; Chen, B.; Pang, R.; Vasudevan, V.; Sandler, M.; Howard, A.; and Le, Q. V. 2019. Mnasnet: Platform-aware neural architecture search for mobile. In *Proceedings of the IEEE Conference on Computer Vision and Pattern Recognition (CVPR)*, 2820–2828.

Xie, S.; Zheng, H.; Liu, C.; and Lin, L. 2018. SNAS: stochastic neural architecture search. In *International Conference on Learning Representations (ICLR)*.

Xu, Y.; Xie, L.; Zhang, X.; Chen, X.; Qi, G.; Tian, Q.; and Xiong, H. 2020. PC-DARTS: Partial Channel Connections for Memory-Efficient Architecture Search. In *International Conference on Learning Representations (ICLR)*.

Zhang, M.; Li, H.; Pan, S.; Chang, X.; and Su, S. 2020. Overcoming multi-model forgetting in one-shot NAS with diversity maximization. In *Proceedings of the IEEE Conference on Computer Vision and Pattern Recognition (CVPR)*, 7809–7818.

Zhong, Z.; Yan, J.; Wu, W.; Shao, J.; and Liu, C.-L. 2018. Practical block-wise neural network architecture generation. In *Proceedings of the IEEE Conference on Computer Vision and Pattern Recognition (CVPR)*, 2423–2432.

Zoph, B.; and Le, Q. V. 2017. Neural architecture search with reinforcement learning. In *International Conference on Learning Representations (ICLR)*.

Zoph, B.; Vasudevan, V.; Shlens, J.; and Le, Q. V. 2018. Learning transferable architectures for scalable image recognition. In *Proceedings of the IEEE Conference on Computer Vision and Pattern Recognition (CVPR)*, 8697–8710.